TAO, Vol. 14, No. 2, 159-182, June 2003

A comprehensive 3D seismic velocity model for the eastern Taiwan-southernmost Ryukyu regions

Yvonne Font[1,*], Honn Kao[2], Char-Shine Liu[3], and Ling-Yun Chiao[3]

(Manuscript received 28 May 2002, in final form 9 April 2003)

ABSTRACT

We describe the construction of a 3D seismic velocity model that may serve as a reference for geophysical investigations in eastern Taiwan, where the westernmost Ryukyu subduction zone connects to the active arc-continent collision zone. For offshore region where local tomography is not available, we construct the model by integrating multiple geophysical data sources in order to characterize, in geometry as well as in velocity, the different structures existing in the area. The multiple data sources used to create the offshore model mainly consist of seismic reflection and refraction data to identify crustal structures and a global hypocenter dataset to define the subduction geometry. The offshore velocity model is then combined with a local onland tomography model in order to create the new 3D P-velocity model. The structures distinguished in this work include the water layer, sedimentary units (e.g., forearc basins and accretionary prism), the oceanic crustal basement of the Philippine Sea plate, the thickened crust of the Luzon Arc, the subducted Philippine Sea slab, and the curved Ryukyu margin. This investigation results in the first comprehensive Vp velocity model for the region and covers the area from 121.0 – 124.4°E and 22.0 – 25.3°N, with its depth reaching 120 km.

(Key words: 3D velocity model, Westernmost Ryukyu subduction zone, Taiwan.)

1. INTRODUCTION

This paper concerns the construction of a comprehensive 3D seismic velocity model (VM) for the region of eastern Taiwan and its offshore area. Several dense clusters of earthquakes, at shallow to intermediate depths, occur offshore, in the vicinity of the interface between the

[1] Géosciences Azur, Obs. Océanologique Villefranche, Villefranche-sur-Mer, France

[2] Pacific Geoscience Center, Geological Survey of Canada, Sidney, Canada

[3] Institute of Oceanography, National Taiwan University, Taipei, Taiwan, ROC

[*] *corresponding author address*: Dr. Yvonne Font, Géosciences Azur, Obs. Océanologique Villefranche, BP 48, 06235 Villefranche-sur-Mer, France; E-mail: font@obs-vlfr.fr

subducting Philippine Sea Plate (PSP) and the overriding Ryukyu margin (Fig. 1). Despite the fact that these earthquakes attest the tectonic complexity of the transition from oblique subduction to active collision zones (Yeh et al. 1991), previously reported hypocentral locations are often associated with large uncertainties (up to 100 km) and tectonic interpretations differ widely depending on which dataset is used (Lallemand et al. 1997; Kao et al. 1998; Font et al. 1999). Thus, it is necessary to relocate accurately earthquakes in this domain.

Theoretically, the main reasons for earthquake location errors are due to inappropriate earth velocity model, incomplete coverage of seismic stations (inducing bad azimuthal coverage), phase reading errors and clock drifts. In the studied area, earthquakes are not only located outside the Taiwanese seismic network, but also determined with a 1-D VM by the Central Weather Bureau (CWB).

Due to strongly biased station coverage of the local seismic networks, there is no detailed tomographic study of the offshore region east of Taiwan. Fortunately, since 1991, several marine geophysical surveys have collected geophysical data that include swath bathymetry, seismic reflection and refraction profiling in the region. These data sets provide sufficient information about the 3D configuration of the local bathymetry as well as crustal structures. In this paper, we construct for the first time a comprehensive 3D P-wave velocity (Vp) model for the eastern Taiwan and offshore area by integrating all the available information published in the literature. It is the first paper in a series of studies to improve finding the hypocenter location of earthquakes that occur in the southernmost Ryukyu-Taiwan region. Description of the hypocentral determination method, the 3D relocation results, and the corresponding seismotectonic implications will be presented in a manuscript under preparation, thus will not be detailed here.

2. FRAMEWORK

Taiwan is located at the boundary between the Philippine Sea plate (PSP) and the continental margin of the Eurasian plate (EUP). Near Taiwan, the PSP converges toward the EUP at an approximate rate of 8 cm/yr along N306°-N312° (Yu et al. 1997). South of Taiwan, the PSP overrides the South China Sea oceanic lithosphere of the EUP (Fig. 1) along the Manila Trench, while north of Taiwan it subducts beneath the rifted EUP margin (i.e., the Ryukyu margin) along the Ryukyu Trench. East of Taiwan, the Luzon volcanic arc, originated from the Manila subduction system and carried by the northwestward PSP, actively collides against the Eurasian continental margin. The Taiwan orogen is thus regarded as the result of this active collision (e.g., Suppe 1981; Ho 1986).

The westernmost extremity of the Ryukyu Trench terminates onto the Taiwanese active collision zone (Fig. 1). Onland and south of the Ryukyu Trench, the Longitudinal Valley marks the suture zone between the PSP (parts of the Luzon Arc that emerges along the Coastal Range) and the Eurasian continental margin (e.g., Angelier et al. 1997). North of the Ryukyu Trench, the subducted PSP slab is observed beneath northern Taiwan (Kao et al. 1998; Font et al. 1999). In this intricate tectonic setting, the connection between the oblique subduction along the Ryukyu Trench and the active collision along the Longitudinal Valley is not well

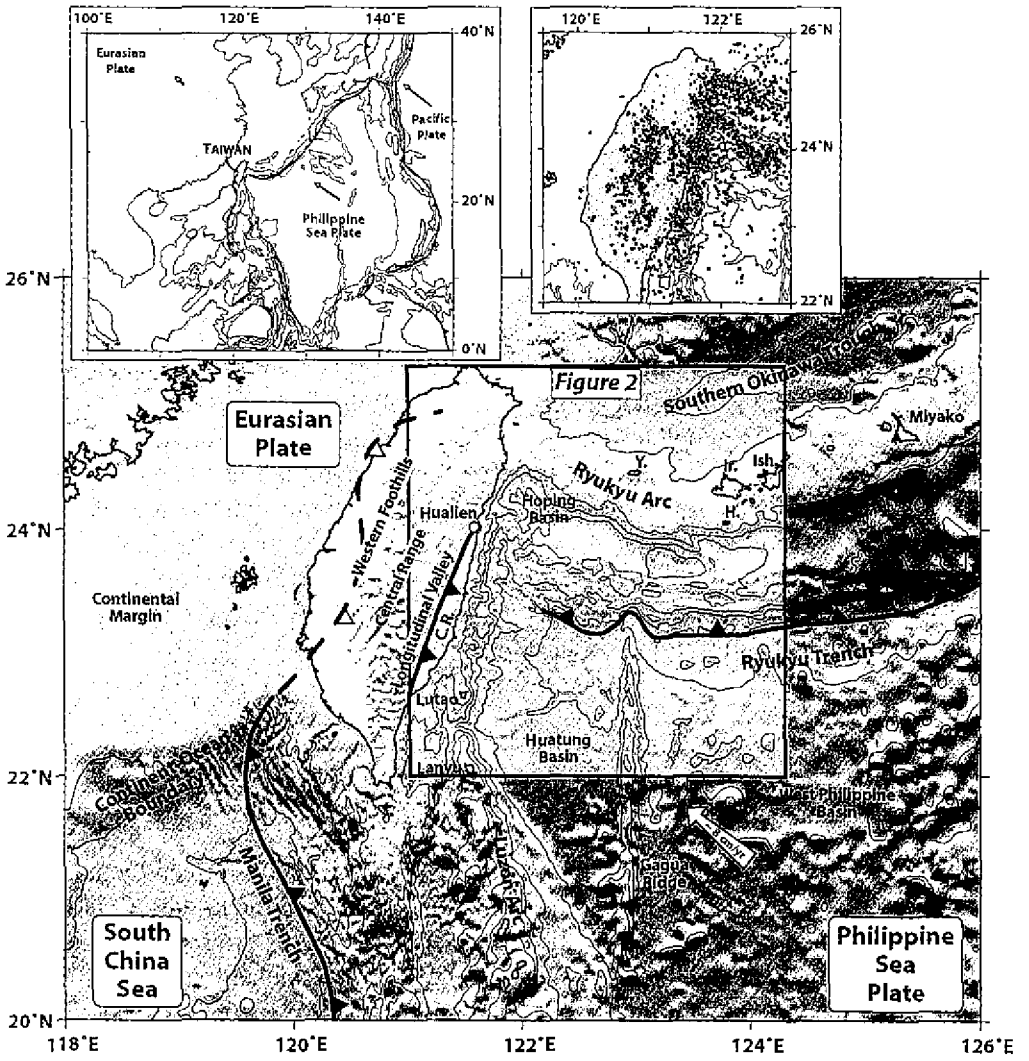

Fig. 1. Geodynamic setting of the Taiwan region. The box bounds the velocity model domain (close-view on Fig. 2). C. R. = Coastal Range; Y = Yonaguni; Ir = Iriomote; Ish = Ishigaki; H = Hateruma. Relative convergence is based on Seno et al. (1993). The upper right view represents seismicity (Mb > 4) from 1991 to 2002 (CWB catalog).

known and the mechanisms of this transition are still controversial (e.g., Angelier et al. 1990; Hsu and Sibuet 1995; Chemenda et al. 1995; 1997; Lallemand et al. 1997; Sibuet and Hsu 1997; Teng 2000; Lallemand et al. 2001). In this domain, several dense earthquake swarms developed (Kao et al. 1998; Font et al. 1999; Kao et al. 2000), over the Okinawa back-arc basin, near the plate interface and along the Coastal Range – Luzon Arc (Fig. 1). To assess properly the tectonic significance revealed by those earthquake swarms and their potential risk

for the nearby population, it is crucial to relocate accurately earthquakes in the eastern Taiwan and offshore areas.

The 3D VM developed in this study covers an area between 121.0 – 124.4°E and 22.0 – 25.3°N, extending over the eastern half of Taiwan, the main seismic clusters offshore eastern Taiwan, and the neighboring Japanese Islands. The model depth reaches 120 km. Within this area, there are ~30 seismic stations installed in eastern Taiwan, and 4 Japanese stations located on Yonaguni, Iriomote, Hateruma and the Ishigaki Islands, respectively (Fig. 1). Offshore eastern Taiwan, we identified major structural entities of the PSP and EUP by characteristics of large Vp gradients. Therefore, the sedimentary layer (essentially composed of forearc basins, accretionary prism and oceanic basin) is distinguished from the crustal basement, and so is the oceanic crust from the upper mantle. South of the Ryukyu Trench, the PSP includes parts of the West Philippine Basin, the Gagua Ridge, the Huatung Basin and the Luzon volcanic arc (Fig. 1). North of the trench, the Ryukyu margin incorporates the Ryukyu accretionary prism, the forearc basins, the Ryukyu Arc and the Okinawa Trough. As a result, the 3D VM shown in this study is probably the most up-to-date representation of the complex tectonic structures in the southernmost Ryukyu-Taiwan region, as it is constrained by all available velocity information in the literature. Consequently, it is not only an essential component for accurate relocation of offshore earthquakes east of Taiwan, but can also serve as a good reference model for future seismological and tectonic studies in the region.

3. DATA

3.1 Onland Tomography

The velocity structure underneath the island of Taiwan is constrained by the tomography model of Rau and Wu (1995) derived from reread and checked the P- and S-phase arrivals of about 1200 selected earthquakes from the CWB Seismic Network original seismograms. Based on their tomographic model, Rau and Wu (1995) observed a thickening of the crust from west to east, with the Moho depth increasing from 25 km under the Western Foothills to 45 km under the Central Range. From south to north, the Moho depth also increases from 40 km at the latitude of Taitung (~22.9°N) to 55 km at the latitude of Taipei (~24.7°N). North of 24.7°N, the 'root' suddenly disappears and the Moho depth shallows to 35 km. In northern Taiwan, a high-velocity zone northward dipping from 20-55 km to 100-130 km in depth coincides with the subducted PSP. A low velocity zone is described at the western extension of the Okinawa Trough, below the Ilan Plain, at depths ranging from 40 to 80 km. Figure 2 shows the extend of the tomography model of Rau and Wu (1995) used in constructing our 3D VM (i.e., between 121.0-121.6°E and 22.0-25.1°N).

3.2 Offshore Active and Passive Experiments

Multiple data sources are compiled in order to define the envelopes of the structural bodies existing in the offshore domain. The consistency among different datasets is carefully checked at the overlapping zones or the intersections between any two models, and the shape

of the envelopes is established in spatial volume. In this section, we summarize the structural geometry information derived from the analyses of bathymetry, seismic reflection and seismic refraction data collected in the last decade (Fig. 2). A few examples are given below to illustrate how various geophysical data are used in VM construction. Nevertheless, the reader is invited to refer to original publications to obtain specific information and details about the acquisition, processing and resolution limits of each dataset. The main structural bodies investigated concern the sedimentary layer and the crustal basement.

3.2.1 Sedimentary layer and top of the crustal basement

The sedimentary layer is delineated by the sea-floor bathymetry envelope and the top of the basement. Large parts of the top of the crustal basement is mapped based on numerous seismic reflection profiles collected from different cruises, including the 1995 EW9505 cruise onboard R/V M. Ewing, the 1996 ACT cruise onboard R/V L'Atalante, and several cruises onboard R/V Ocean Researcher I (Liu, unpublished data; Font 1996; Lallemand et al. 1997; Lallemand et al. 1999; Dominguez et al. 1998; Schnurle et al. 1998a, 1998b; Yang 1999; Font et al. 2001 – Fig. 2 for location). Two main domains are considered: the Ryukyu margin and the Huatung Basin (Fig. 2). In each domain, seismic reflection profiles are tied to their intersections and interpreted. The reflector corresponding to the top of the basement is digitized and mapped. The basement depth map is converted from two-way travel times to km (below sea level) by using a velocity function corresponding to the sedimentary sequence (Font et al. 2001).

In the Ryukyu margin, we observe that the top of the Ryukyu Arc is deflected beneath the Okinawa Trough axis (Fig. 3). It lies at around 6 km deep and is covered by about 3 km of sediments (e.g., Letouzey and Masaaki 1986; Sibuet et al. 1998; Hirata et al. 1991; McIntosh and Nakamura 1999). On top of the arc, the top of the basement follows the bathymetry surface and is covered by less than 200 m of sediments (Schnurle et al. 1998b; Sibuet et al. 1998; Font et al. 1999; Font 2001). Beneath the forearc basins (0.5 to 3 km thick), the top of the arc basement is represented by topographic lows and highs varying approximately between 4 and 9 km in depth (Font et al. 2001). South of the Ryukyu Trench, the top of the PSP is nearly flat beneath the Huatung Basin (covered by 1 to 2 km of sediments) and inflected upward where the Gagua Ridge and Luzon Arc stand (e.g., Schnurle et al. 1998a; C. S. Liu, unpublished data). The top of the crust is deflected north of the Ryukyu Trench, reflecting the curvature of the plate to be subducted and is covered by the thickened accretionary prism (up to 10 km of sediments).

At depth, the top of the subducting PSP is constrained by the global hypocenter dataset issued from Engdahl et al. (1998). These authors improved significantly the global hypocenter determination by using – in addition to regional and teleseismic P and S phases – the arrival times from the inner core and teleseismic depth phases. Nowadays, this dataset is considered to be one of the most accurate global datasets available. East of the Gagua Ridge, the slab shows a moderate 50°-dipping Wadati-Benioff zone down to 280 km. West of the Gagua Ridge, the slab dip increases to 65°, that may reflect the older age of the Huatung Basin (~120 my) compared to the West Philippine Basin (~45 my, Deschamps et al. 2000). Near Taiwan,

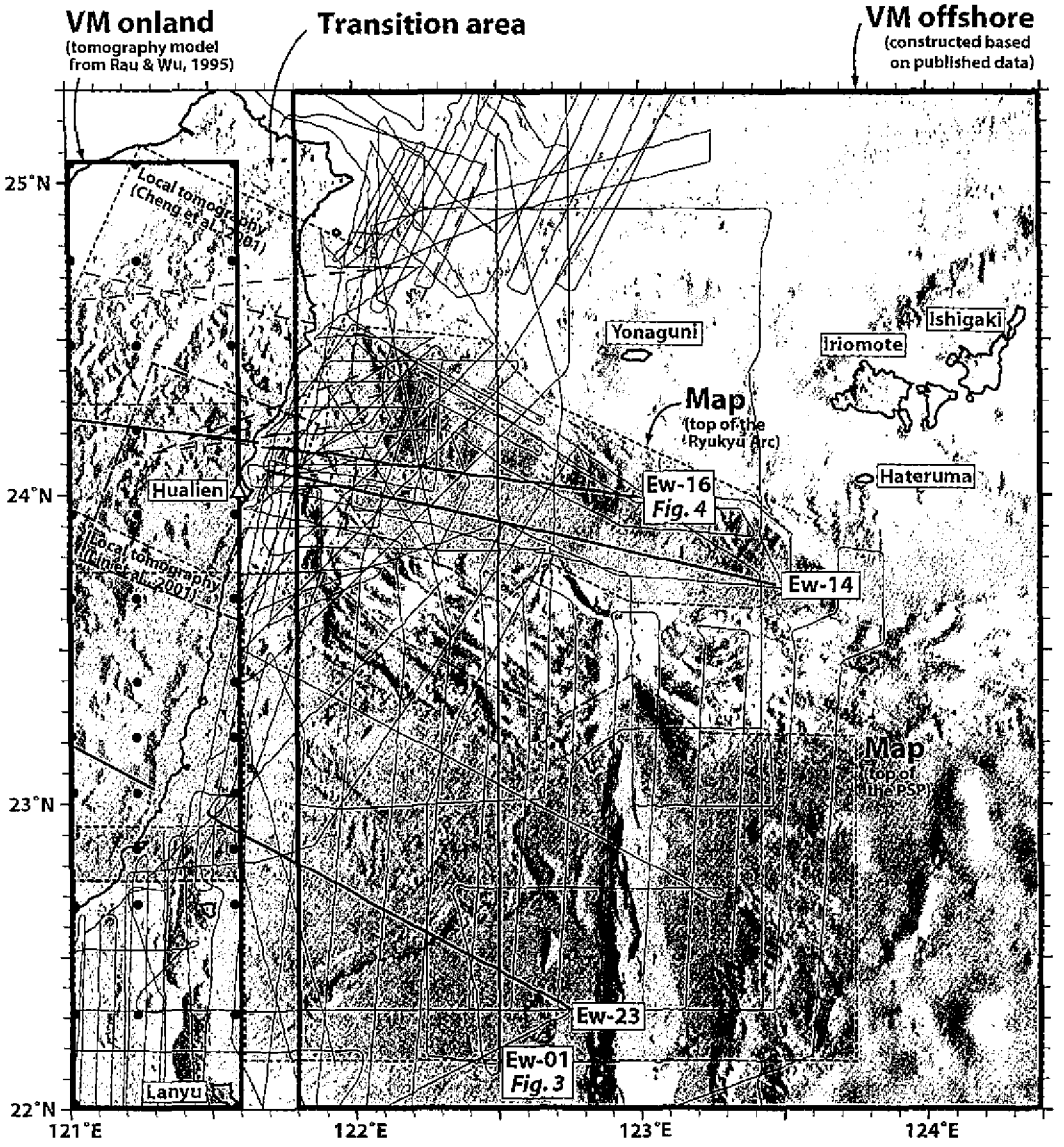

Fig. 2. Coverage of the different data sources existing in the velocity model domain. Bold boxes bound the 2 main velocity domains: the onland tomography model and the constructed offshore velocity model. Black dots represent onland tomography data nodes. Onland dashed box bounds local tomography models. Offshore dashed boxes limit the maps of the Ryukyu Arc top (Font et al. 1999) and the PSP top. Thin lines show the locations of seismic reflection profiles. Bold lines represent the main refraction profiles (collected during the TAICRUST project), while dash lines represent older refraction profiles.

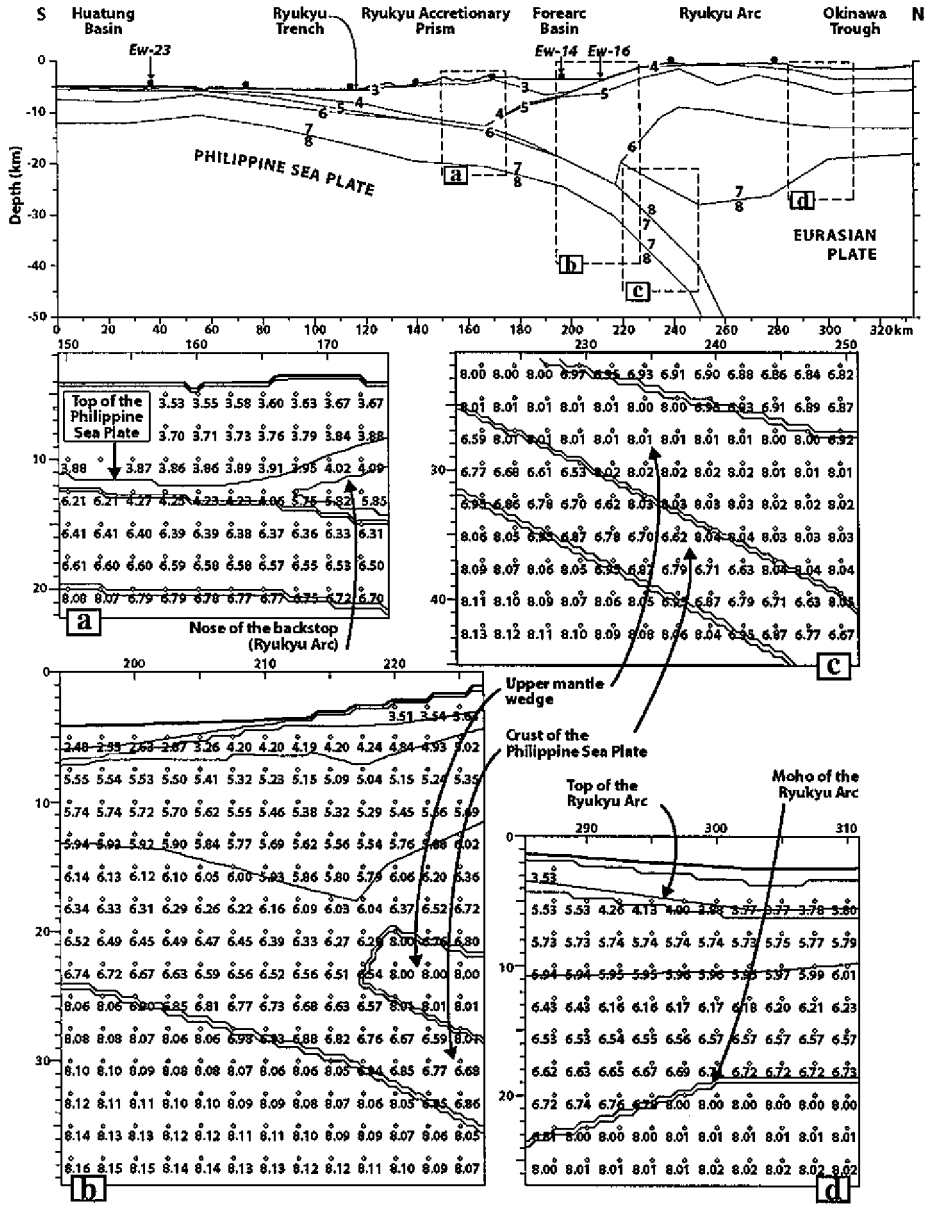

Fig. 3. Simplified seismic refraction model along line Ew-01 (from McIntosh and Nakamura 1999). See location on Fig. 2. Data points presented in boxes a, b, c and d are issued from the gridded refraction model.

the slab shows a steep 70° subducting lithosphere down to 300 km.

3.2.2 Thickness of the crustal basement

The thickness of the basement (sediments excluded) is deduced from the refraction profiles acquired in the area (Fig. 2 for location). A N-S trending profile located near the eastern edge of the VM indicates that the EUP crustal thickness decreases to 12 km beneath the Okinawa Trough axis, with the Moho lying at a depth of about 18 km (Hirata et al. 1991). The crust thickens to 25 km across the Ryukyu Arc and decreases again to ~20 km above the mantle wedge (McIntosh and Nakamura 1999; line Ew-01 – Figs. 2 and 3). The thickness of the Ryukyu margin crust decreases gradually until its southernmost extremity is reached. Along two E-W profiles running across the forearc basins (Wang and Chiang 1998; McIntosh and Nakamura 1998), the crustal thickness of the Ryukyu Arc varies from 11 to 18 km, with an average of around 15 km. South of the Ryukyu Trench, the WNW-ESE trending refraction profile Ew-23 (Yang and Wang 1998; Yang 1999) and the N-S line Ew-01 (McIntosh and Nakamura 1999; Wang and Pan 2001) indicate that the PSP crust in the Huatung Basin is about 7 km thick, with the Moho discontinuity lying at about 12 km below sea level (Fig. 3). West of 122°N, the crust thickens rapidly as it approaches the Luzon Arc.

At depth, the thickness of the subducting PSP is observed from a 400 km-long refraction line normal to the Ryukyu Trench (Line Ew-01, McIntosh and Nakamura 1999; Wang and Pan 2001 – Figs. 2 and 3). The crustal thickness varies from 6 to 9 km, with the Moho roughly parallel to the top of the crust. Both seismic refraction results and global hypocenter dataset (Engdahl et al. 1998) are compatible in delineating the top of the PSP. Based on an E-W profile running along the southern foot of the Ryukyu Arc (refraction line Ew-16), the average crustal thickness of the PSP below the EUP crust is 7.5 km (Wang and Chiang 1998).

3.3 Data Consistency in the Transition Area

In order to link the velocity structures derived from onland tomography model (Rau and Wu 1995) and the offshore offshore reflection/refraction results, we define a "transition area" in our VM that connects the Vp onland and offshore Taiwan. This transition area extends between 121.5 and 121.8°E (Fig. 2). The connection between onshore and offshore models needs particular consideration for 3 main reasons. First, no single dataset covers the totality of the transition area and consequently the structures that extend in this region are only with difficultly distinguished as a whole entity. Second, the transition area is intended to connect two models that are based on different data sources. This implies that Vp on each edge of the transition area (western and eastern sides) may – or may not – be inconsistent. The junction therefore needs to be examined particularly in order to avoid strong lateral heterogeneities triggered by the original dataset inconsistencies rather than the real structures. Third, specific and intricate crustal structures develop in the transition area. The following chapter illustrates the special attention that has been paid to check the data consistency and to construct velocity structures of two particular regions in the transition area: (1) along the Luzon Arc and the Coastal Range and (2) near the Hualien area and Hsincheng Ridge.

3.3.1 Crustal thickness of the Luzon Arc

The northern extremity of the Luzon Arc is observed around 24°N. South of this latitude, the Luzon Arc develops in a nearly N-S direction (Figs. 1 and 2). The velocity model of the arc is poorly resolved, especially at depth, because both sides of the area are constrained by the edges of the respective models (tomography and refraction). Furthermore, the transition area covers most of the Luzon Arc, where the crust is probably the thickest (e.g., Yeh et al. 1998). Nevertheless, no consistent velocity data are reliable along the Luzon Arc axis, and consequently the crustal thickness (and associated Vp) needs to be derived by interpolation of different data sources.

Onland, Cheng et al. (2001) constructed tomographic models for 4 sub-areas of the Taiwan Island (Fig. 2). The authors observed a high velocity anomaly in the middle and lower crust between the Central Range and the Luzon Arc. This observation is comparable with the tomography model of Rau and Wu (1995). North of Lanyu Island (Fig. 2), the western Luzon Arc is generally associated with relatively low Vp (compared to the Central Range – Cheng et al. 2001). Around 23°N where the refraction line Ew-23 terminates, the Moho discontinuity (marked by the 7.5 km s^{-1} Vp contour) is observed at 55 km depth. Rau and Wu's tomography model also shows high velocity gradients (the 8 km s-1 Vp contour) at a similar depth range (52-57 km). The Moho discontinuity dips gently eastward, which probably reflects the fact that the crust is slightly thicker than 55 km beneath the Luzon Arc. Both tomography models are consistent in pattern, but the VM of Rau and Wu (1995) shows systematically higher Vp values than that of Cheng et al. (2001).

Offshore, the OBS seismic refraction line Ew-23 is not well resolved at its western termination because few seismic rays penetrate beneath the Moho at the edges of this model (Yang 1999). The same refraction line analyzed from onland data (Hetland and Wu 2001) shows that the Moho (here at ~8 km s^{-1}) reaches 35 km depth beneath the eastern part of the Luzon Arc. The rapid westward deepening of the 8 km s^{-1} velocity contour indicates that the Moho could reach greater depth beneath the Luzon Arc.

In summary, the depth of the Moho increases rapidly from the Huatung Basin (12.5 km deep, at 121.7°N) to the Luzon Arc-Coastal Range. The crust of the Luzon Arc is estimated to be over 50 km thick. However, because the velocity gradient associated with the Moho discontinuity varies from one data source to the other, it is difficult to estimate precisely the crustal thickness beneath the arc axis. To tie both onland and offshore VMs, we choose to respect the Vp values given by the onland tomography. Therefore, the strong velocity gradient (from 7 to 8 km s^{-1} in about 1 km in vertical distance) observed on the offshore refraction profiles is gradually disminished in the transition area so that the Vp contours match the onland tomography values, on one hand, and preserve the thickened crustal observed beneath the Luzon Arc, on the other hand.

3.3.2 Low velocity zone beneath the Hsincheng Ridge

The region surrounding Hualien city shows one of the most intricate seismogenic patterns in the Taiwan area (e.g., Kao et al. 2001). This area is the site where the Ryukyu Arc terminates by the collision belt. A thick layer (at least 6 km) of sediments is observed in the Hoping

forearc basin (about 50 km northeast offshore Hualien – Fig. 1) where the Ryukyu basement is at 9 km depth, and even deeper beneath the Hsincheng Ridge (Font et al. 1999). The transition from this large basement low to the collision belt (Eurasian plate) happens in less than 30 km in horizontal distance and is poorly understood, especially at depth. The tomography model from Rau and Wu (1995) does not cover this region, thus other geophysical data are examined to connect the Vp from the onland collision zone to the offshore subduction zone.

Onland and at these latitudes, a cross-section along the onshore continuation of the refraction profile Ew-16 (Figs. 1 and 4) is realized within the tomography results of Rau and Wu (1995). All velocity contours present an upward inflection around 121.5°N (Fig. 4), indicating that a high velocity zone may exist below the eastern Central Range immediately west of the Hsincheng Ridge. This high velocity zone is also observed on the local tomography model of Lin et al. (1998) as a 10 to 15 km wide feature. This feature seems to be continuous from the near surface to a depth of about 35 km. A relatively low velocity body (lower than 6 km s^{-1}) bounds the high velocity zone to the east, reaching at least 20 km in depth after Lin et al. (1998) and about 30 km after Chen et al. (2001). This low velocity zone extends beneath the Hsincheng Ridge.

The offshore OBS refraction line Ew-16 (Wang and Chiang 1998) can not resolve the velocity structures near its western edge, but additional information is provided by onland data of the same profile (Hetland and Wu 2001 – Fig. 4). Relatively low Vp (lower than 5 km s^{-1}) is

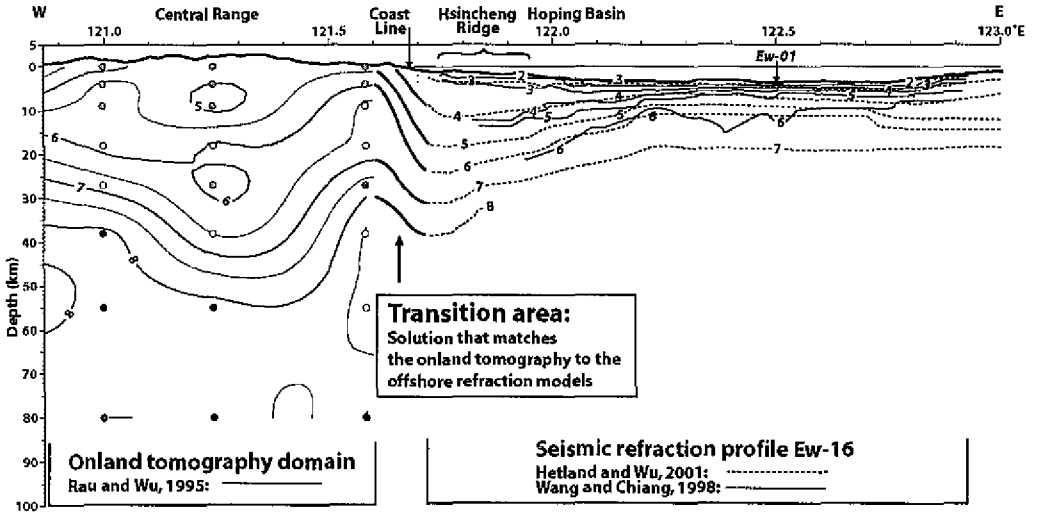

Fig. 4. E-W section approximately along the onland continuation of the seismic refraction line Ew-16 (Fig. 2). The onland tomography Vp contours from Rau and Wu (1995) are represented west of 121.6°E. Refraction models are represented on the offshore area (east of 121.7°N). Bold lines between 121.6 and 121.75°E represent the transition area that matches the offshore and onshore models.

observed beneath the Hsincheng Ridge (Hetland and Wu 2001) with Vp contours deflected down to 20 km until they reach the eastern edge of the Central Range where they suddenly tilt upward.

In summary, a low velocity body characterizes the Hsincheng Ridge - Hoping Basin area where Vp contours are deflected down to at least 30 km. This low velocity anomaly is bounded to the west by a high velocity zone. The transition area coincides with the transition between these 2 structures, and velocity contours in this domain dip eastward connecting the onland tomography to the offshore VM (Fig. 4).

4. CONSTRUCTION OF THE P-VELOCITY MODEL

The construction of the whole VM basically resides in tying the existing onland tomography model to the constructed offshore VM with a proper interpolation within the transition area. Due to the poor seismic ray-path coverage and the lack of seismic stations, seismic tomography can not be well constrained in the area offshore eastern Taiwan and especially at depth (Hsu 2001). The main difficulty therefore consists in building the offshore VM (between 121.8-121.4°E and 22.0-25.3°N) where geophysical constrains are scattered and resolving Vp inconsistencies between different models.

4.1 P-waves Velocity Values

In the offshore domain, we deduce Vp data from 3 different sources: (1) Velocity of the sedimentary layer is derived from multi-channel seismic reflection data (Font et al. 1999); (2) crustal Vp are obtained from seismic refraction data (Hirata et al. 1991; Cheng et al. 1996; Hagen et al. 1998; Hetland and Wu 1998; McIntosh and Nakamura 1998; Wang and Chiang 1998; Yang and Wang 1998; McIntosh and Nakamura 1999; Yang 1999; Hetland and Wu 2001; Wang and Pan 2001); (3) below the Moho discontinuity, the earth model iasp91 (Kennett and Engdahl 1991) provides the Vp data.

Several difficulties arise when combining different data sources to create a VM. The main one is that the strict correlation between Vp and structural interfaces (i.e., envelopes) does not always exist. For example, at the plate interface south of the mantle wedge (Fig. 3b), the interface corresponding to the top of the subducting PSP is difficult to distinguish from the relatively high Vp values of the Ryukyu lower crust and the subducting PSP crust. In such a case, the structural interface has to be extrapolated from strong lateral velocity gradient. On the other hand, a Vp discontinuity does not always represent a unique structural interface. A typical example is the 4 km s^{-1} Vp contour that corresponds to the nose of the Ryukyu Arc backstop turning into the top of the subducted PSP further south (Fig. 3a). Another major difficulty is that Vp values do not necessarily fit at the intersection between two models, and compromises have to be reached in these cases. We briefly summarize the Vp data available in the offshore domain and present the average Vp value that best approximates each structural interface.

Detailed velocity analyses are performed along the Ew-14 reflection profile running across the Ryukyu forearc sedimentary basins (Font et al. 1999). About 30 velocity functions have

been determined at every 500 CDP (~6 km) along the profile. We observed that deformation of sediments does not modify significantly the velocity functions at different locations; the velocity data seem to depend mainly on compaction of sediments (i.e., depth of burial). Because of the similarity of the 30 Vp functions, we then deduced an average velocity function representing the sedimentary velocity of the region.

North of the Ryukyu Trench, the Vp value at the top of the Ryukyu Arc basement varies between 3 and 5 km s^{-1} (McIntosh and Nakamura 1999 – Fig. 3d). The seismic velocity of this interface is often associated with a sharp gradient from 4 to ~5 km s^{-1} in less than 500 m in vertical distance. The average Vp is then approximated to 4.5 km s^{-1} over the Ryukyu Margin. The Moho discontinuity is represented by the 7 to 8.1 km s^{-1} velocity gradient (in less than 1 km in vertical distance). The Vp gradient within the Ryukyu Arc basement is not uniform, and the geometry of the 5 and 6 km s^{-1} Vp iso-contours is taken into consideration to reflect this gradient in the VM (from Line Ew-01, McIntosh et Nakamura 1999). South of the Ryukyu Trench, the Vp value at the top of the PSP crust is about 4.8 km s^{-1} and is considered constant over this domain. The Vp increases gradually to 6.5 km s^{-1} at 40 km depth (top of the subducted slab – Fig. 3). Those results are in agreement with other refraction experiments across the Northern and Middle Ryukyu Trench (e.g., Iwasaki et al. 1990; Kodaira et al. 1996). Within the PSP, Vp values gradually increase from a value ranging between 4.8 and 6.5 km s^{-1} (depending on the depth of the top surface) to 7 km s^{-1} immediately above the Moho discontinuity. The Moho discontinuity itself is represented by a strong velocity gradient from 7 to 8.1 km s^{-1} in less than 1 km of vertical distance, excepted in the transition area.

4.2 Construction Method

After resolving the Vp inconsistencies among the multiple geophysical data sources, the first step in the construction of the VM for the offshore domain is to delineate the main structural surfaces (Fig. 5a). The detailed bathymetry is obtained after the ACT cruise (Lallemand et al. 1997; Liu et al. 1998). The surface corresponding to the top of the crustal basements has been mapped where the coverage of the seismic reflection profiles was adequate, allowing us to model the Ryukyu forearc and the Huatung sedimentary basins. The Wadati-Benioff zone is constrained based on a series of 2-D cross sections through the Engdahl et al. (1998) hypocenter dataset, and the top of the subducting plate surface is mapped laterally from the Japanese Islands to its western extremity beneath northern Taiwan. We then constructed a series of 2-D cross sections (16 N-S and 8 E-W sections, Fig. 5a) spaced at every 0.2° that allow us to map the complex configuration of the Ryukyu arc-forearc-trench system. The Vp attributed to each structural envelope are shown in Table 1.

The envelopes of constant Vp reported on each cross-section are digitized (Fig. 5b), and lateral extrapolation is first performed to complete each structural interface. We consequently obtain a set of surfaces, defined by spatial points (x, y and z) associated with a constant velocity (Vp). We proceed with lateral and vertical extrapolation (respectively) of the data points to acquire a consistently spaced set of grid nodes. The lateral extrapolation consists of averaging all values included in blocks of $10 \times 10 \times 3$ km in dimension. Because nodes are closely distributed near the surface, lateral extrapolation results in a set of averaged values equally spaced on

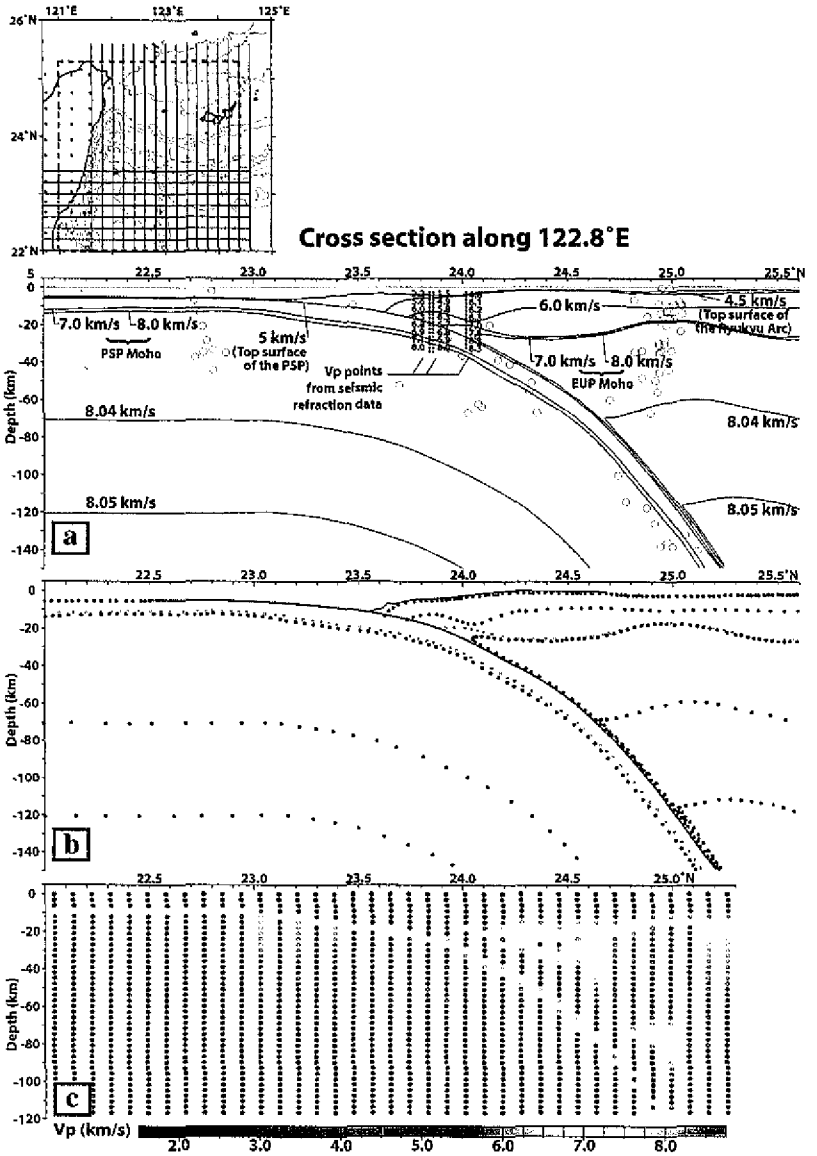

Fig. 5. Example of the constant Vp envelopes constructed along a N-S cross-section. The map (top of the figure) illustrates the location of the 24 sections where a similar work is done. (a) Drawing of the iso-Vp contours based on the existing velocity and structural data (see text for more details). (b) Digitalization of the envelopes drawn in step A. The top of the PSP slab surface is created based on the earthquake hypocenter dataset of Engdahl et al. (1998), and the top of the Ryukyu Arc surface is based on a seismic reflection study of Font et al. (1999). (c) Resulting velocity model after extrapolation.

Table 1. Vp and thickness corresponding to the interfaces of different layers appeared in the 3D velocity model. PSP = Philippine Sea Plate; SOT =South Okinawa Trough.

Surface or layer	Vp (km/s)	Thickness of surface or layer
Bathymetry	1.55	-
Top of the PSP	5.00	8 km
Moho PSP	7 to 8	2 km in vertical distance
Top Ryukyu Arc	4.5	depending on location: ~25 km beneath the arc; 12-15 km beneath SOT
Moho Ryukyu Arc	7 to 8 (excepted at termination of upper mantle wedge)	2 km in vertical distance
Upper Mantle	8.04 at 70 km depth	-
	8.05 at 120 km depth	-

the horizontal layers close to the sea-level and the crustal structures (including the water column). Beneath the Moho, only few Vp nodes exist and vertical extrapolation is needed to fill-up the empty grid-points. Finally, the onland tomography data file is extrapolated into an equally spaced data set and combined with the offshore model (Fig. 5c).

5. RESULTS AND DISCUSSION

This study presents the first 3D velocity model of the tectonically complex region of eastern Taiwan and its offshore area. This VM is constructed by integrating Vp constraints from different data sources. Techniques have been developed to smooth out the discrepancies among different data sources along their intersections. The resulting VM is coherent with the tectonic domains of eastern Taiwan as it reflects the main structural characteristics existing in the region (Fig. 6). Offshore, the water layer is included. The model respects the contortions of the slab observed on the hypocenter dataset of Engdahl et al. (1998), particularly along the northern extension of the Gagua Ridge (Fig. 6a - Font et al. 1999). The oceanic crust of the PSP is thickened to 40-50 km at depth as it approaches the Luzon Arc (Fig. 6b). Meanwhile, the curved configuration of the Ryukyu margin and the associated lateral variations as it approaches Taiwan from the neighboring Japanese islands are also apparent in the model.

In more details, one can see that the extrapolation method applied to the data set has considerably smoothed the low velocity gradients, and thus only strong heterogeneities prevail. South of the Ryukyu Trench, the top of PSP basement, digitized at 5 km s^{-1}, has been averaged with low velocity values of the sedimentary sequences lying above. Consequently, the Vp value associated with the top of PSP surface tends to be lower in the resulting VM, and closer to the value indicated by seismic refraction constraints (4.8 km s^{-1}). Beneath the mantle wedge of the Ryukyu margin, the extrapolation combines the 5 km s^{-1} of the PSP top surface with the relatively high Vp values of the EUP lower crust and upper mantle, so that the top surface of PSP is closer to 6 km s^{-1}, which was originally observed (e.g., Fig. 6c). In any case, constant Vp along the structural interfaces does not exist, and instead, structural boundaries are well

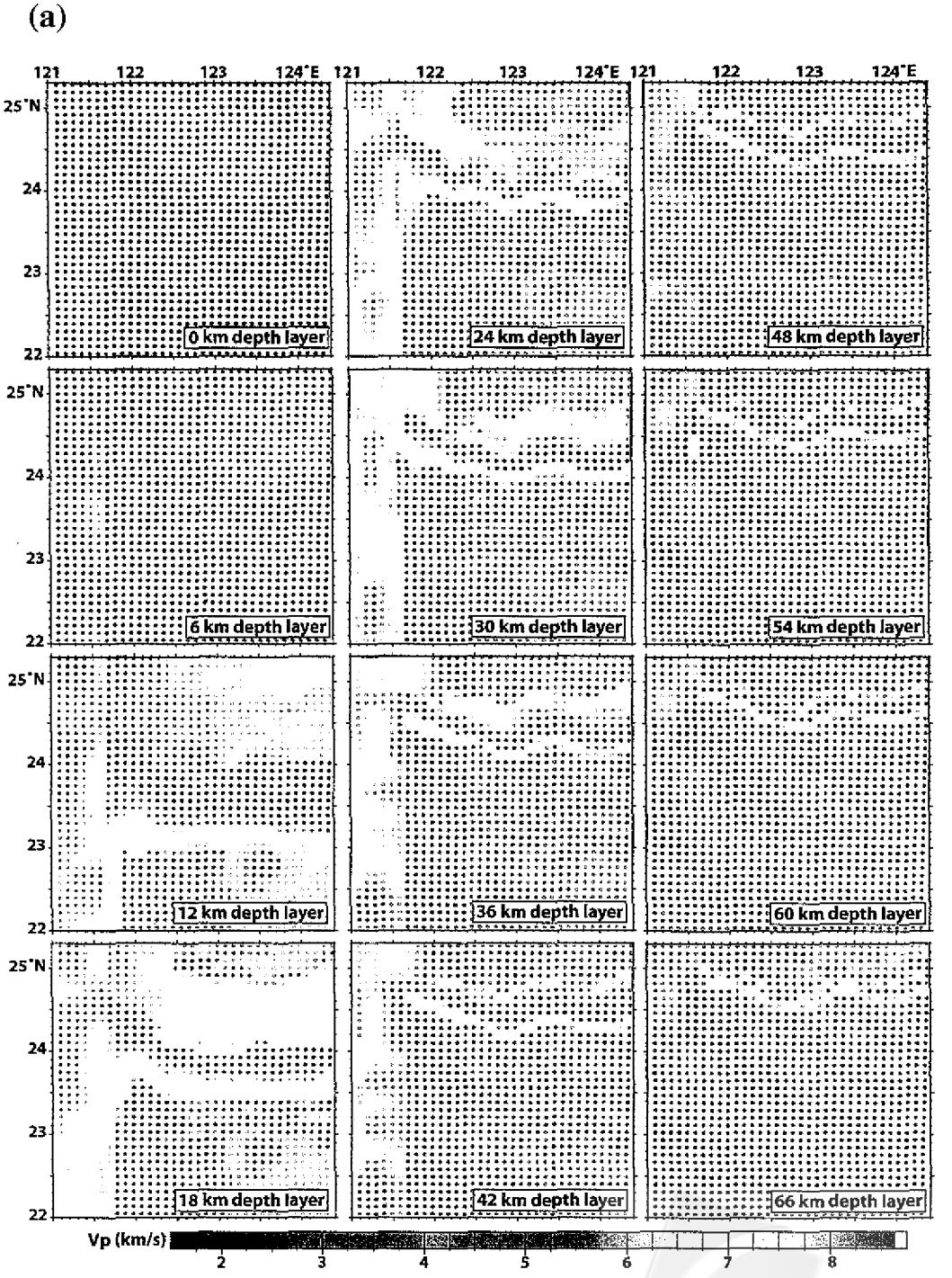
(a)
121
122
123
124°E
25°N
24
23
22
0 km depth layer
24 km depth layer
48 km depth layer
6 km depth layer
30 km depth layer
54 km depth layer
12 km depth layer
36 km depth layer
60 km depth layer
18 km depth layer
42 km depth layer
66 km depth layer
Vp (km/s)
2
3
4
5
6
7
8

(b)

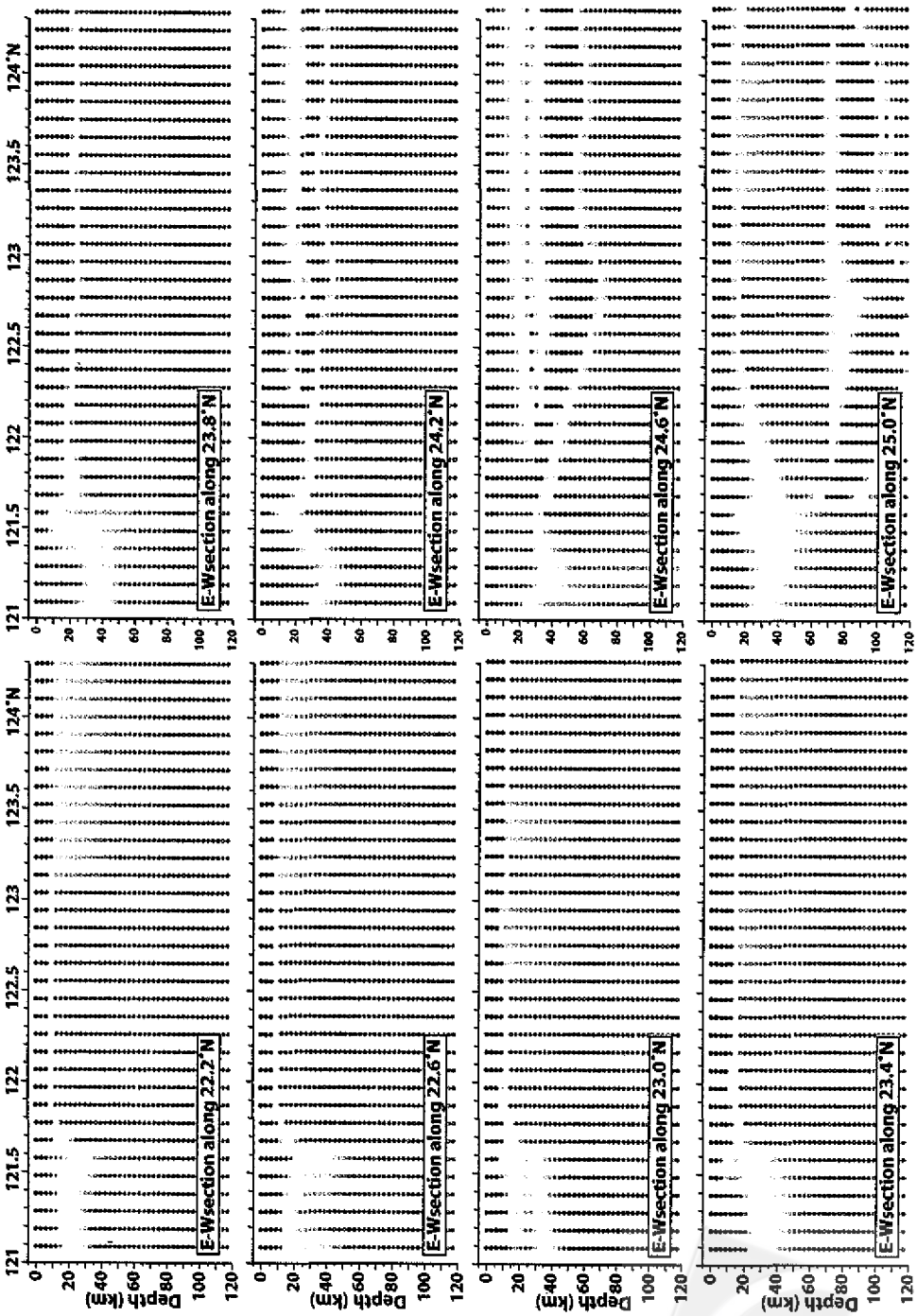
E-Wsection along 22.2°N
E-Wsection along 22.6°N
E-Wsection along 23.0°N
E-Wsection along 23.4°N
E-Wsection along 23.8°N
E-Wsection along 24.2°N
E-Wsection along 24.6°N
E-Wsection along 25.0°N
Depth (km)
Vp (km/s)

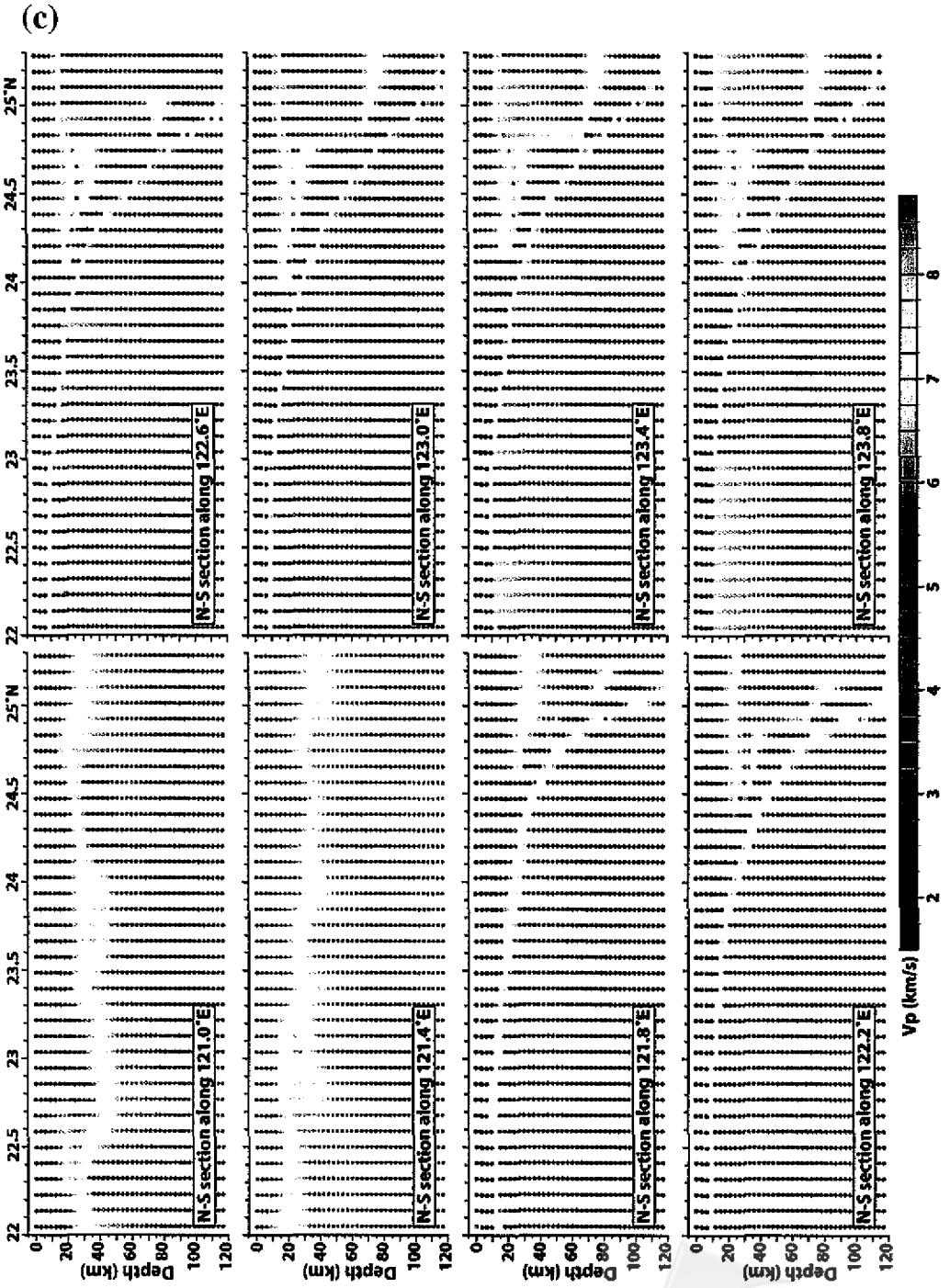

Fig. 6. Cross-sections within the 3D velocity model. (a) Horizontal sections. (b) Along E-W direction. (c) Along N-S direction.

represented by strong velocity gradients.

There are a few aspects in the model that deserve further discussion. One of them concerns the systematic larger Vp values inherited from the tomographic result of Rau and Wu (1995) compared to that derived from the offshore refraction models. Despite the efforts brought within the transition area, it still results in a near vertical discontinuity along 121.7°E (Figs. 6a, b). Fortunately, the lateral heterogeneity of this discontinuity occurs generally at depths greater than 50 km and is usually not strong (from 7.8 to 8.0 km s^{-1} in 20 km of horizontal distance). Locally, between 24.2 and 24.6°N (visible on E-W sections, Fig. 6b), the velocity change can reach 0.4 km s^{-1} in less than 15 km horizontally due to the very high Vp associated with the subducted slab in the onland tomography model (~9.0 km s^{-1}, after Rau and Wu 1995). Because the onland tomography model from Rau and Wu (1995) presents higher Vp values compared to onland-offshore refraction models, one way to improve the VM is to test other onland tomography datasets. For example, the tomography solution of Chen (1995) presents smaller lateral velocity contrasts in the transition area that might reduce velocity discrepancies between onland and offshore VMs.

Near the surface, the water layer should equally be adjusted to the coastline to avoid an inappropriate lateral heterogeneity (Fig. 6a). However, such adjustment should be made carefully, particularly in the southern part of the VM where the onland tomography model covers parts of the water layer. Since a tomography model is the best solution issued from inversion of seismic data, if parts of the model are altered, the Vp values in other paths of the model might loose their significance.

In conclusion, this study demonstrates an alternative way of obtaining a 3D velocity model in a region where seismic ray path coverage is insufficient to establish a reliable tomographic image of the crust and upper mantle. Though the quality of each model used in this study is difficult to estimate quantitatively, this is the first comprehensive 3D velocity model for the eastern Taiwan and its offshore area. Because the construction of the VM respects the geometry and Vp values associated with different structural bodies, we can consequently infer that the 3D VM certainly well approximates the Earth in eastern Taiwan region. The 3D VM presented in this study can serve as a good reference model for future tectonic studies in the region but also can provide an essential component for specific geophysical investigations. An absolute hypocentral location process performed with a 3D algorithm (the Maximum Intersection method) and based on observed arrival times from CWB and Japanese meteorological Agency combined networks, has been conducted eastern Taiwan using the 3D VM presented in this paper (Fig. 7). As a quality proof for the VM, the earthquake clusterization and the significant drop in residual statistics (from 1.20 to 0.35 s, for CWB catalog and 3D-relocation solutions, respectively) attest to the accuracy of the VM constructed in the eastern Taiwan region.

Acknowledgements The Ministry of Education, R.O.C., through the Bureau de Representation de Taipei en France, kindly provided a 4-year long scholarship to the first author. This research was funded by the National Science Council to C. S. Liu through the grants NSC85-2611-M-002-005Y, NSC86-2117-M-002a-001-ODP, NSC87-2611-M-002A-016-ODP, NSC88-2611-M-002-024-ODP and NSC89-2611-M-002-013-ODP, and to H. Kao through the grants NSC89-2921-M-001-012-EAF and NSC89-2116-M-001-017. The first author also

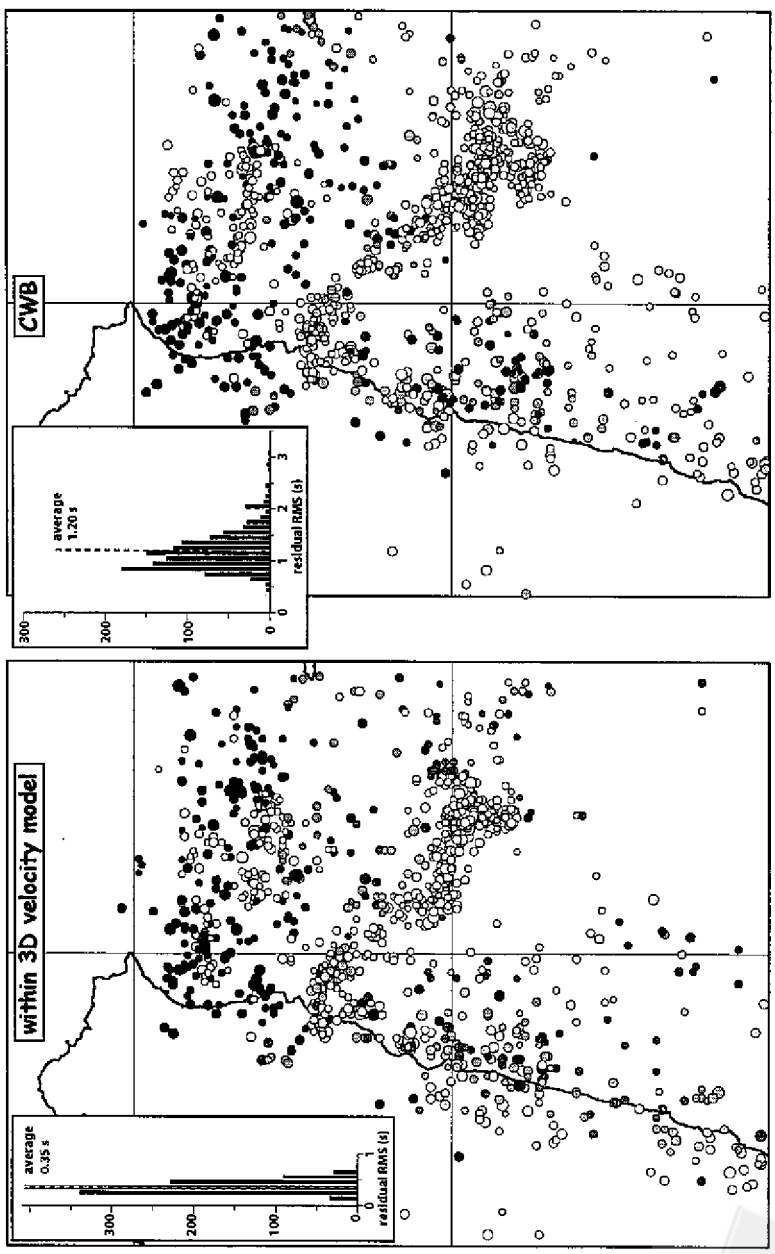

Fig. 7. Hypocentral determinations and associated residual histogram for the CWB solutions and earthquakes relocated within the 3D VM constructed in this study.

thanks the Fundacio Credit Andorra for their support. Both the National Science Council (R. O.C.) and the French Institute in Taipei support the France-Taiwan cooperation program in Earth Sciences. We thank the captains, crews and technical staffs of the R/Vs Ocean Researcher I, Maurice Ewing and L'Atalante for their help in collecting the seismic data used in this study. Win-Bin Cheng, Yen-Lin Chen, Shih Ruey-Chyuan, Bob Engdahl, Eric Hetland, Shu-Kun Hsu, Kirk McIntosh, Ruey-Juin Rau, Tan-Kin Wang, Francis Wu, Y. S. Yang. provided advice and/or data used in this investigation. Most of the figures were generated using the GMT software of Wessel and Smith (1995). Authors also thank Philippe Schnurle for providing the map of the top of the PSP map south of the Ruykyu Trench and Frédéric Masson and Serge Lallemand for their advice and scientific discussions. Ruey-Juin Rau and the anonymous reviewer are thanked for their valuable comments on the manuscript.

REFERENCES

Angelier, J., F. Bergerat, H. T. Chu, and T. Q. Lee, 1990: Tectonic analysis and the evolution of a curved collision belt: the Hsuehshan Range, northern Taiwan. *Tectonphysics*, **183** (1-4), 77-96.

Angelier, J., H. T. Chu, and J. C. Lee, 1997: Shear concentration in a collision zone: kinematics of the Chihshang Fault as revealed by outcrop-scale quantification of active faulting, Longitudinal Valley, eastern Taiwan. *Tectonophysics*, **274**, 117-143.

Chemenda, A. I., M. Mattauer, and A. N. Bokun, 1995: A mechanism for syn-collisional deep rock exhumation and associated normal faulting: results from physical modeling. *Earth Planet Sci. Lett.*, **132**, 225-232.

Chemenda, A. I., R. K. Yang, C. H. Hsieh, and A. L. Groholsky, 1997: Evolutionary model for the Taiwan collision based on physical modelling. *Tectonophysics*, **274**(1-3), 253-274.

Chen, Y. L., 1995: Three-dimensional velocity structure and kinematics analysis in Taiwan area. Master Thesis (in Chinese with English abstract), National Central University, Chung-Li, 172 pp.

Chen, Y. L., and T. C. Shin, 1998: Study on the earthquake location of 3-D velocity structure in the Taiwan area. *Meteo. Bull.*, **42**, 135-169.

Cheng, W. B., C. Wang, and C. T. Shyu, 1996: Crustal structure of the northeastern Taiwan area from seismic refraction data and its tectonic implications. *Terr. Atm. Ocean. Sci.*, **7**(4), 467-487.

Cheng, W. B., C. Wang, C. T. Shyu, and T. C. Shin, 2001: Crustal structure of the convergent plate-boundary zone, eastern Taiwan, assessed by seismic tomography. *Geological Soc. Amer. Bull.*, in press.

Deschamps, A., P. Monie, S. Lallemand, S. K. Hsu, and K. Y. Yeh, 2000: Evidence for Early Cretaceous oceanic crust trapped in the Philippine Sea Plate. *Earth Planet. Sci. Lett.*, **179**, 503-516.

Dominguez, S., S. Lallemand, J. Malavieille, and P. Schnurle, 1998: Oblique subduction of the Gagua Ridge beneath the Ryukyu accretionary wedge system - Insight from marine observations and sandbox experiments. *Mar. Geophys. Res.*, **20**(5), 383-402.

Engdahl, E. R., R. D. Van Der Hilst, and R. Buland, 1998: Global teleseismic earthquake relocation with improved travel times and procedures for depth relocation. *Bull. Seismol. Soc. Am.*, **88**, 722-743.

Font, 2001: Modes of the ongoing arc-continent collisional processes in Taiwan: new insights from seismic reflection analyses and earthquake relocation. Ph. D. Thesis, National Taiwan University, 281 pp; defended on September 24th 2001.

Font, Y., 1996: Etude de la sismicite au nord-est de Taiwan: consequences sur la deformation de la plaque Philippine au front de la zone de collision. Diplome d'Etude Approfondies Thesis, Universite de Montpellier, Montpellier, France, 46 pp.

Font, Y., S. Lallemand, and J. Angelier, 1999: Etude de la transition entre l'orogene actif de Taiwan et la subduction des Ryukyu - Apports de la sismicite. *Bull. Soc. Geol. France* (in French with extended English abstract), **170**(3), 271-283.

Font, Y., C. S. Liu, P. Schnurle, and S. Lallemand, 2001: Constraints on Backstop Geometry from the Southwest Ryukyu Subduction based on Reflection Seismic Data. *Tectonophysics*, **333**, 135-158.

Hagen, R. A., F. K. Duennebier, and V. Hsu, 1988: A seismic refraction study of the crustal structure in the active seismic zone east of Taiwan. *J. Geophys. Res.*, **93**(5), 4785-4796.

Hetland, E., and F. Wu, 2001: Crustal structure at the intersection of the Ryukyu Trench with the arc-continent collision in Taiwan: Results from offshore-onshore seismic experiment. *Terr. Atm. Ocean. Sci.*, **12**, 231-248.

Hetland, E. A., and F. T. Wu, 1998: Deformation of the Philippine Sea Plate under the Coastal Range, Taiwan: Results from offshore-onshore seismic experiment. *Terr. Atm. Ocean. Sci.*, **9**(4), 363-378.

Hirata, N., N. Hirata, H. Kinoshita, H. Kattao, H. Baba, Y. Kaiho, S. Koresawa, Y. Ono, and K. Hayashi, 1991: Report on DELP 1988 Cruises in the Okinwa Trough. Part 3. Crustal structure of the southernn Okinawa Trough. *Bull. Earth Res. Inst. Univ. Tokyo*, **66**, 37-70.

Ho, C. S., 1986: A synthesis of the geologic evolution of Taiwan. *Tectonophysics*, **125**, 1-16.

Hsu, S. K., 2001: Subduction/collision complexities in the Taiwan-Ryukyu junction area: Tectonics of the northwestern corner of the Philippine Sea Plate. *Terr. Atm. Ocean. Sci.*, **Suppl. Issue**, 209-230.

Hsu, S. K., and J. C. Sibuet, 1995: Is Taiwan the result of arc-continent or arc-arc collision? *Earth Planet Sci. Lett.*, 136(3-4), 315-324.

Iwasaki, T., N. Hirata, T. Kanazawa, J. Melles, K. Suyehiro, T. Urabe, L. Moller, J. Makris, and H. Shimamura, 1990: Crustal and upper mantle structure in the Ryukyu Island Arc deduced from deep seismic sounding. *Geophys. J. Int.*, **102**, 631-651.

Kao, H., G. C. Huang, and C. S. Liu, 2000: Transition from oblique subduction to collision in the northern Luzon arc - Taiwan region: Constraints from bathymetry and seismic observations. *J. Geophys. Res.*, **105**, 3059-3079.

Kao, H., S. S. Shen, and K. F. Ma, 1998: Transition from oblique subduction to collision: Earthquakes in the southernmost Ryukyu arc-Taiwan region. *J. Geophys. Res.*, **103**, 7211-7229.

Kao, H., and P. R. Jian, 2001: Seismogenic patterns in the Taiwan region: Insights from

source parameter inversion of BATS data. *Tectonophysics*, **333**, 179-198.

Kennett, B. L. N. and E. R. Engdahl, 1991: Travel times for global earthquake location and phase identification. *Geophys. J. Int.*, **105**, 429-465.

Kodaira, S., T. Iwasaki, T. Urabe, T. Kanazawa, F. Egloff, J. Makris, and H. Shimamura, 1996: Crustal structure across the middle Ryukyu Trench obtained from ocean bottom seismographic data. *Tectonophysics*, **263**(1-4), 39-60.

Lallemand, S., Y. Font, H. Bijwaard, and H. Kao, 2001: New insights on 3D plates interaction near Taiwan from tomography and tectonic implications. *Tectonophysics*, **335**, 229-253.

Lallemand, S., C. S. Liu, S. Dominguez, P. Schnurle, J. Malavieille, and the A. C. T. scientific crew, 1999: Trench-parallel stretching and folding of forearc basins and lateral migration of the accretionary wedge in the southern Ryukyus: A case of strain partition caused by oblique convergence. *Tectonics*, **18**(2), 231-247.

Lallemand, S., C. S. Liu, J. Angelier, J. Y. Collot, B. Deffontaines, S. Dominguez, M. Founier, S. K. Hsu, J. P. Le Formal, S. Y. Liu, C. Y. Lu, J. Malavieille, P. Schnurle, J. C. Sibuet, N. Thareau, and F. Wang, 1997: Swath Bathymetry reveals active arc-continent collision near Taiwan. *EOS*, **78**(17), 173-175.

Lee, W. H. K., and S. W. Stweart, 1981: Principle and Application of Microearthquake Network. Academic Press, New York.

Letouzey, J., and M. Kimura, 1986: The Okinawa trough: Genesis of back-arc basin developing along a continental margin. *Tectonophysics*, **125**, 209-230.

Lin, C. H., Y. H. Yeh, H. Y. Yen, K. C. Chen, B. S. Huang, S. W. Roecker, and J. M. Chiu, 1998: Three-dimensional elastic wave velocity structure of the Hualien region of Taiwan: Evidence of active crustal exhumation. *Tectonics*, **17**(1), 89-103.

Liu, C. S., S. Y. Liu, S. Lallemand, N. Lundberg, and D. Reed, 1998: Digital elevation model and its tectonic implications. *Terr. Atm. Ocean. Sci.*, **9**(4), 705-738.

McIntosh, K., and Y. Nakamura, 1998: Crustal structure beneath the Nanao forearc basin from TAICRUST MCS/OBS Line 14. *Terr. Atm. Ocean. Sci.*, **9**(3), 345-362.

McIntosh, K., and Y. Nakamura, 1999: Structure and Tectonics offshore south and east of Taiwan: Same results of the TAICRUST MCS/OBS survey. In: M. Geosciences-Montpellier (Editor), SEASIA conference, Montpellier.

Rau, R. J., and F. T. Wu, 1995: Tomographic imaging of lithospheric structures under Taiwan. *Earth. Planet. Sci. Lett.*, **133**, 517-532.

Schnurle, P., C. S. Liu, S. Lallemand, and D. Reed, 1998a: Structural controls of the Taitung Canyon in the Huatung basin east of Taiwan. *Terr. Atm. Ocean. Sci.*, **9**(3), 453-472.

Schnurle, P., C. S. Liu, S. Lallemand, and D. Reed, 1998b: Structural insight into the south Ryukyu margin: Effects of the subducting Gagua Ridge. *Tectonophysics*, **288**, 237-250.

Seno, T., S. Stein, and A. E. Gripp, 1993: A model for the motion of the Philippine Sea Plate with NUVEL-1 and geological data. *J. Geophys. Res.*, **98**, 17941-17948.

Sibuet, J. C., B. Deffontaines, S. K. Hsu, N. Thareau, J. P. Le Formal, C. S. Liu, and the A. C. T. party, 1998: Okinawa Trough back-arc basin: Early tectonic and magmatic evolution. *J. Geophys. Res.*, **103**, 30245-30267.

Sibuet, J. C., and S. K. Hsu, 1997: Geodynamics of Taiwan arc-arc collision. *Tectonophysics*, **274**, 221-251.

Suppe, J., 1981: Mechanics of mountain building in Taiwan. *Mem. Geol. Soc. China*, **4**, 67-89.

Teng, L. S., C. Lee, Y. Tsai, and L. Y. Hsiao, 2000: Slab breakoff as a mechanism for flipping of subduction polarity in Taiwan. *Geology*, **28**(2), 155-158.

Wang, T. K., and C. H. Chiang, 1998: Imaging of arc-arc collision in the Ryukyu forearc region offshore Hualien from TAICRUST OBS line 16. *Terr. Atmos. Ocean. Sci.*, **9**(3), 329-344.

Wang, T. K., and C. H. Pan, 2001: Crustal Poisson's ratio off Eastern Taiwan from OBS data modeling. *Terr. Atm. Ocean. Sci.*, **12**, 249-269.

Wessel, P., and W. H. F. Smith, 1995: New Version of the Generic Mapping Tools Released. *EOS Trans*, **76**, 329.

Yang, Y. S., 1999: Crustal velocities of the Huatung Basin from refracted and reflected data. Master Thesis, National Taiwan Ocean University, Keelung, (in Chinese) 91 pp.

Yang, Y. S., and T. K. Wang, 1998: Crustal velocity variation of the western Philippine Sea Plate from TAICRUST OBS/MCS Line 23. *Terr. Atm. Ocean. Sci.*, **9**(3), 379-393.

Yeh, Y. H., R. C. Shih, C. H. Lin, C. C. Liu, H. Y. Yen, B. S. Huang, C. S. Liu, P. Z. Chen, C. S. Huang, C. J. Wu, and F. T. Wu, 1998: Onshore/Offshore wide-angle deep seismic profiling in Taiwan. *Terr. Atm. Ocean. Sci.*, **9**(3), 301-316.

Yeh, Y. H., E. Barrier, C. H. Lin, and J. Angelier, 1991: Stress tensor analysis in the Taiwan area from focal mechanisms of earthquakes. *Tectonophysics*, **200**, 267-280.

Yu, S. B., H. Y. Chen, and L. C. Kuo, 1997: Velocity field of GPS stations in the Taiwan area. *Tectonophysics*, **274**, 41-59.

APPENDIX A

The 3D velocity model constructed in this study is 350×370×120 km, along the E-W (x), N-S (y) and depth (z) directions, respectively. The SW corner is assigned to be the origin point and is located at 120.95°E, 22.00°N and 0 km depth. The heterogeneous velocity structures are characterized with a set of non-overlapping, equal volume and constant velocity blocks. Each block dimension is 10×10×3 km in x, y and z direction. The Vp-node is located at the center of each block. The velocity model therefore consists in 35×37×40 = 51,800 nodes. Here is an example of the digital file. Please contact the corresponding author to access the whole model (font@dstu.univ-montp2.fr).

Note: ix and iy should be multiplicated by 10 to obtain the x and y coordinates in km; iz should be multiplicated by 3 to obtain the z value.

Vp	ix	iy	iz																				
				1.51	190	10	0	4.46	50	30	0	1.50	260	40	0	1.50	120	60	0	1.50	330	70	0
				1.54	200	10	0	4.44	60	30	0	1.50	270	40	0	1.50	130	60	0	1.50	340	70	0
4.79	0	0	0	1.50	210	10	0	1.54	70	30	0	1.50	280	40	0	1.50	140	60	0	4.06	0	80	0
4.60	10	0	0	1.50	220	10	0	1.50	80	30	0	1.50	290	40	0	1.50	150	60	0	3.92	10	80	0
4.41	20	0	0	1.50	230	10	0	1.50	90	30	0	1.50	300	40	0	1.50	160	60	0	3.78	20	80	0
4.47	30	0	0	1.50	240	10	0	1.50	100	30	0	1.50	310	40	0	1.50	170	60	0	3.80	30	80	0
4.76	40	0	0	1.50	250	10	0	1.50	110	30	0	1.50	320	40	0	1.50	180	60	0	3.99	40	80	0
5.05	50	0	0	1.50	260	10	0	1.50	120	30	0	1.50	330	40	0	1.50	190	60	0	4.18	50	80	0
5.31	60	0	0	1.50	270	10	0	1.50	130	30	0	1.50	340	40	0	1.50	200	60	0	4.34	60	80	0
2.85	70	0	0	1.50	280	10	0	1.50	140	30	0	3.88	0	50	0	1.50	210	60	0	1.54	70	80	0
1.54	80	0	0	1.50	290	10	0	1.50	150	30	0	3.90	10	50	0	1.50	220	60	0	1.50	80	80	0
1.50	90	0	0	1.50	300	10	0	1.50	160	30	0	3.91	20	50	0	1.50	230	60	0	1.50	90	80	0
1.50	100	0	0	1.50	310	10	0	1.50	170	30	0	3.99	30	50	0	1.50	240	60	0	1.50	100	80	0
1.50	110	0	0	1.50	320	10	0	1.50	180	30	0	4.12	40	50	0	1.50	250	60	0	1.50	110	80	0
1.50	120	0	0	1.50	330	10	0	1.51	190	30	0	4.25	50	50	0	1.50	260	60	0	1.50	120	80	0
1.50	130	0	0	1.50	340	10	0	1.54	200	30	0	4.35	60	50	0	1.50	270	60	0	1.50	130	80	0
1.50	140	0	0	4.41	0	20	0	1.50	210	30	0	1.50	70	50	0	1.50	280	60	0	1.50	140	80	0
1.50	150	0	0	4.39	10	20	0	1.50	220	30	0	1.50	80	50	0	1.50	290	60	0	1.50	150	80	0
1.50	160	0	0	4.38	20	20	0	1.50	230	30	0	1.50	90	50	0	1.50	300	60	0	1.50	160	80	0
1.50	170	0	0	4.43	30	20	0	1.50	240	30	0	1.50	100	50	0	1.50	310	60	0	1.50	170	80	0
1.50	180	0	0	4.55	40	20	0	1.50	250	30	0	1.50	110	50	0	1.50	320	60	0	1.50	180	80	0
1.51	190	0	0	4.66	50	20	0	1.50	260	30	0	1.50	120	50	0	1.50	330	60	0	1.50	190	80	0
1.54	200	0	0	4.72	60	20	0	1.50	270	30	0	1.50	130	50	0	1.50	340	60	0	1.50	200	80	0
1.50	210	0	0	1.54	70	20	0	1.50	280	30	0	1.50	140	50	0	3.53	0	70	0	1.50	210	80	0
1.50	220	0	0	1.50	80	20	0	1.50	290	30	0	1.50	150	50	0	3.50	10	70	0	1.50	220	80	0
1.50	230	0	0	1.50	90	20	0	1.50	300	30	0	1.50	160	50	0	3.46	20	70	0	1.50	230	80	0
1.50	240	0	0	1.50	100	20	0	1.50	310	30	0	1.50	170	50	0	3.56	30	70	0	1.50	240	80	0
1.50	250	0	0	1.50	110	20	0	1.50	320	30	0	1.50	180	50	0	3.80	40	70	0	1.50	250	80	0
1.50	260	0	0	1.50	120	20	0	1.50	330	30	0	1.51	190	50	0	4.03	50	70	0	1.50	260	80	0
1.50	270	0	0	1.50	130	20	0	1.50	340	30	0	1.54	200	50	0	4.24	60	70	0	1.50	270	80	0
1.50	280	0	0	1.50	140	20	0	4.05	0	40	0	1.50	210	50	0	1.54	70	70	0	1.50	280	80	0
1.50	290	0	0	1.50	150	20	0	4.09	10	40	0	1.50	220	50	0	1.50	80	70	0	1.50	290	80	0
1.50	300	0	0	1.50	160	20	0	4.14	20	40	0	1.50	230	50	0	1.50	90	70	0	1.50	300	80	0
1.50	310	0	0	1.50	170	20	0	4.20	30	40	0	1.50	240	50	0	1.50	100	70	0	1.50	310	80	0
1.50	320	0	0	1.50	180	20	0	4.28	40	40	0	1.50	250	50	0	1.50	110	70	0	1.50	320	80	0
1.50	330	0	0	1.51	190	20	0	4.35	50	40	0	1.50	260	50	0	1.50	120	70	0	1.50	330	80	0
1.50	340	0	0	1.54	200	20	0	4.38	60	40	0	1.50	270	50	0	1.50	130	70	0	1.50	340	80	0
4.60	0	10	0	1.50	210	20	0	1.50	70	40	0	1.50	280	50	0	1.50	140	70	0	4.60	0	90	0
4.50	10	10	0	1.50	220	20	0	1.50	80	40	0	1.50	290	50	0	1.50	150	70	0	4.36	10	90	0
4.39	20	10	0	1.50	230	20	0	1.50	90	40	0	1.50	300	50	0	1.50	160	70	0	4.11	20	90	0
4.44	30	10	0	1.50	240	20	0	1.50	100	40	0	1.50	310	50	0	1.50	170	70	0	4.06	30	90	0
4.65	40	10	0	1.50	250	20	0	1.50	110	40	0	1.50	320	50	0	1.50	180	70	0	4.19	40	90	0
4.86	50	10	0	1.50	260	20	0	1.50	120	40	0	1.50	330	50	0	1.50	190	70	0	4.33	50	90	0
5.02	60	10	0	1.50	270	20	0	1.50	130	40	0	1.50	340	50	0	1.50	200	70	0	4.41	60	90	0
2.57	70	10	0	1.50	280	20	0	1.50	140	40	0	3.71	0	60	0	1.50	210	70	0	1.54	70	90	0
1.50	80	10	0	1.50	290	20	0	1.50	150	40	0	3.70	10	60	0	1.50	220	70	0	1.50	80	90	0
1.50	90	10	0	1.50	300	20	0	1.50	160	40	0	3.69	20	60	0	1.50	230	70	0	1.50	90	90	0
1.50	100	10	0	1.50	310	20	0	1.50	170	40	0	3.77	30	60	0	1.50	240	70	0	1.50	100	90	0
1.50	110	10	0	1.50	320	20	0	1.50	180	40	0	3.96	40	60	0	1.50	250	70	0	1.50	110	90	0
1.50	120	10	0	1.50	330	20	0	1.51	190	40	0	4.15	50	60	0	1.50	260	70	0	1.50	120	90	0
1.50	130	10	0	1.50	340	20	0	1.54	200	40	0	4.30	60	60	0	1.50	270	70	0	1.50	130	90	0
1.50	140	10	0	4.23	0	30	0	1.50	210	40	0	1.50	70	60	0	1.50	280	70	0	1.50	140	90	0
1.50	150	10	0	4.29	10	30	0	1.50	220	40	0	1.50	80	60	0	1.50	290	70	0	1.50	150	90	0
1.50	160	10	0	4.36	20	30	0	1.50	230	40	0	1.50	90	60	0	1.50	300	70	0	1.50	160	90	0
1.50	170	10	0	4.40	30	30	0	1.50	240	40	0	1.50	100	60	0	1.50	310	70	0	1.50	170	90	0
1.50	180	10	0	4.43	40	30	0	1.50	250	40	0	1.50	110	60	0	1.50	320	70	0	1.50	180	90	0